International Journal of Microwave and Wireless Technologies

cambridge.org/mrf

Dual-polarized, monostatic antenna array with improved T_x–R_x isolation for 2.4 GHz in-band full duplex applications

Haq Nawaz, Ahmad Umar Niazi, M. Abdul Basit, Furqan Shaukat and Muhammad Usman

Electronics Engineering, University of Engineering and Technology (UET) Taxila, Sub-Campus Chakwal, 48800, Chakwal, Pakistan

Research Paper

Cite this article: Nawaz H, Niazi AU, Basit MA, Shaukat F, Usman M (2020). Dual-polarized, monostatic antenna array with improved T_x–R_x isolation for 2.4 GHz in-band full duplex applications. *International Journal of Microwave and Wireless Technologies* **12**, 398–408. https://doi.org/10.1017/S1759078719001569

Received: 6 June 2019
Revised: 19 November 2019
Accepted: 20 November 2019
First published online: 6 January 2020

Key words:
Dual polarized patch antenna array; improved interport isolation; in-band full duplex; self interference cancellation (SIC)

Author for correspondence:
Haq Nawaz,
E-mail: haq.nawaz@uettaxila.edu.pk

Abstract

This paper presents a two-elements based, dual polarized, single layer, patch antenna array with improved isolation between transmit (T_x) and receive (R_x) ports for 2.4 GHz in-band full duplex (IBFD) or simultaneous transmit and receive wireless applications. The differential feeding deployed at the R_x port effectively suppresses the coupling which is termed as self-interference from the T_x port to achieve high T_x–R_x interport isolation. A simple 3 dB/180° ring hybrid coupler with nice amplitude and phase balance characteristics has been used for differential R_x operation. The mathematical description for a differential feeding based self-interference cancellation mechanism is also presented for the proposed dual polarized IBFD antenna array. The measurement results for the implemented prototype of the antenna array demonstrate very nice levels of T_x–R_x interport isolation. The implemented single layer, compact antenna array presents 10 dB return-loss bandwidth of more than 50 MHz for both T_x and R_x ports. The prototype achieves >80 dB peak interport isolation and 75 dB (65 dB) isolation in 20 MHz (50 MHz) bandwidth.

Introduction

The improved spectral efficiency is one of the major goals/requirements for next generation wireless networks (5 G) to achieve higher data rates or throughputs. The in-band full duplex (IBFD) also termed as single channel full duplex transceivers based on monostatic antenna architecture (same antenna for transmit-T_x and receive-R_x operation) has the potential of theoretically doubling the spectral efficiency compared to conventional time and frequency duplexing schemes [1–6]. Furthermore, the simultaneous transmit and receive (STAR) operation in the same range of frequencies can resolve several issues effectively in conventional wireless communication networks and commercial of the shelf multi-in multi-out (MIMO) transceivers can be used for the implementation of STAR transceivers [7, 8].

In conventional frequency division duplexing systems based on single antenna architecture, a duplexer is employed in order to separate T_x and R_x signals. However, the conventional duplexers cannot be used for IBFD operation as the interport isolation of such duplexer is severely degraded when transmission and reception is accomplished at the same frequencies as indicated in Fig. 1. The resulting very large amount of self-interference (SI) from transmitter (T_x) to its own receiver (R_x) is the major issue which hinders the practical realization of IBFD wireless communication [1–3]. The high power SI signal overpowers the very weak received signal of interest (SOI) and results in severe degradation in signal to noise ratio (SNR) for intended wireless link [9]. These high power SI signals are comprised of both linear and non-linear components resulting from direct coupling between T_x and R_x chains in addition to SI generated from environmental reflections or nearby objects [10].

An effective mechanism to suppress the SI which is usually termed as self-interference cancellation (SIC) is required on R_x side to retrieve the SOI for successful IBFD communication [9, 10]. Normally a large amount of SIC is required to suppress the SI to receiver's noise floor. These intended SIC levels are defined by radiated power (transmit power), noise figure (NF), and bandwidth of IBFD transceiver [9]. For example, as computed below, >110 dB SIC is required for a radio transceiver transmitting +20 dBm power (P_T), 20 MHz bandwidth (B.W), and NF of 11 dB for such transceiver [9]:

$$\begin{aligned}\text{Noise floor } (P_N) &= -174\,\text{dBm} + 10\log(\text{B.W}) + \text{NF} \\ &= -174\,\text{dBm} + 73 + 11 = -90\,\text{dBm}\end{aligned} \tag{1}$$

$$\text{Required SIC Levels} = P_T - P_N = 20 + 90 = 110\,\text{dB} \tag{2}$$

© Cambridge University Press and the European Microwave Association 2020

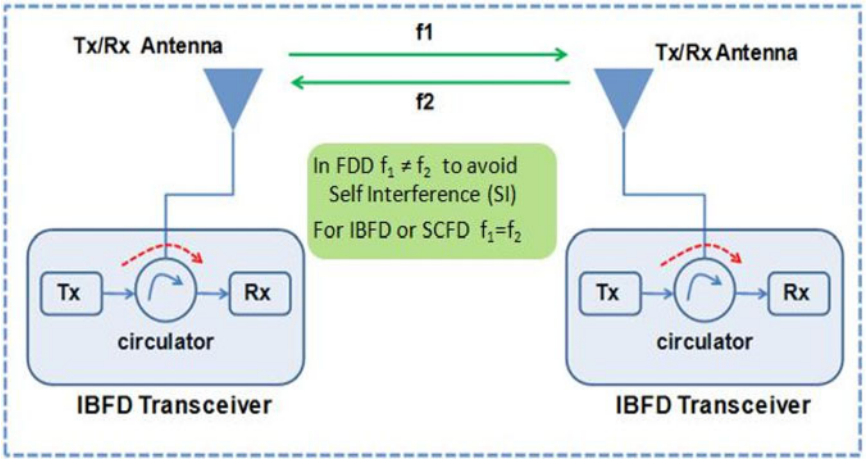


Fig. 1. IBFD wireless communication through STAR operation at the same frequency by using a monostatic antenna configuration.

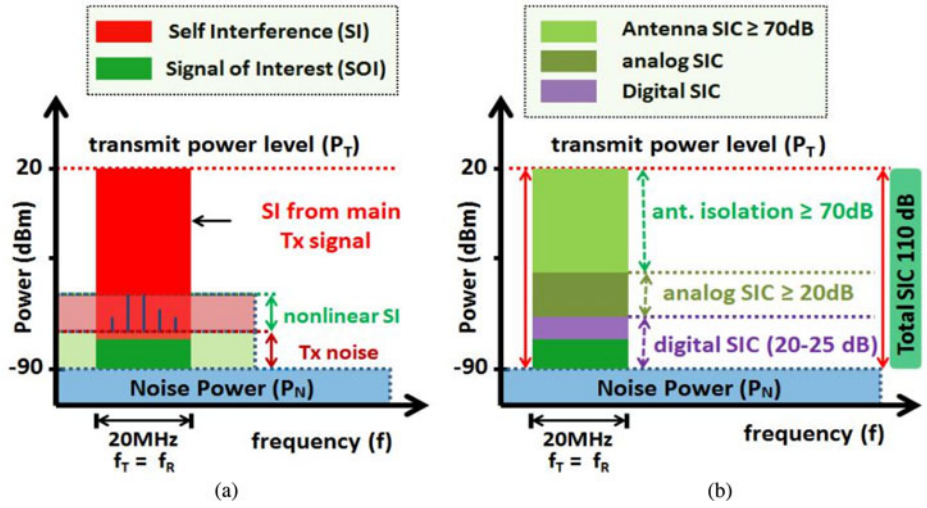


Fig. 2. (a) SI components (b) around 110 dB SIC for the monostatic antenna based transceiver when antenna interport isolation ≥70 dB within 20 MHz bandwidth.

The SIC levels stated in (2) are intended to fully suppress the SI to the receiver's noise floor (−90 dBm for this example as illustrated in Fig. 2). As clear from (2), required SIC levels are directly related to T_x power i.e. high T_x power levels require more SIC to realize IBFD operation. Conversely, a low T_x power can relax the required amount of SIC, however, the reduced T_x power will decrease the range or coverage of wireless transmitter.

These high levels of required isolation can be accomplished through multiple SIC topologies which can be deployed at various stages across the IBFD transceiver [11]. Normally, theses topologies utilize SIC at an antenna stage and techniques based on SIC in an analog/radio frequency (RF) and digital baseband domain [12] as illustrated in Fig. 2. Moreover, a comparatively high amount of SIC is required at receiver's front end to prevent the saturation of the receive chain from very strong SI signals [10, 13]. In addition, a monostatic antenna with high interport isolation plays a critical role in achieving required SIC levels for the realization of a compact transceiver as it alleviates the SIC requirements at subsequent stages. In general, time or frequency based digital domain SIC techniques offer 20–25 dB SIC levels [14, 15]. Moreover, a single-tap, signal inversion based analog/RF domain can achieve >20 dB isolation within 20 MHz bandwidth for the monostatic antenna configuration. Thus, exploiting a monostatic antenna capable of providing 65–70 dB interport isolation plays a vital role in achieving required SIC levels of 110–115 dB for the IBFD transceiver based on monostatic antenna architecture as illustrated in Fig. 2. Moreover, such a high interport isolation antenna at transceiver's front end can provide flexibility of deploying additional SIC stages for improved T_x–R_x isolation, especially, for high T_x power cases where more SIC levels are required as obvious from (2). Furthermore, the use of a monostatic IBFD antenna array provides improved gain to extend the coverage and reliability of communication link for specified receiver's sensitivity under given SNR values without additional SIC requirements at the R_x side of the IBFD transceiver.

Although, the bistatic antenna configuration (separate antenna elements for T_x and R_x operation) can be deployed with the IBFD transceiver where the inter-antenna spacing (spatial isolation) achieves the reduced coupling between T_x and R_x channels. In addition, the T_x and R_x operation can be performed with orthogonal polarization to achieve improved propagation domain isolation through the polarization diversity mechanism. However, deploying separate antenna elements for T_x and R_x operation weakens the real motive of IBFD topology as the bistatic antenna configuration itself can improve the throughput of conventional half duplex MIMO (multi-input multi-output) systems [16]. Furthermore, the bistatic antenna configuration requires more spacing (especially for improved T_x–R_x isolation) which impedes

https://doi.org/10.1017/S1759078719001569 Published online by Cambridge University Press

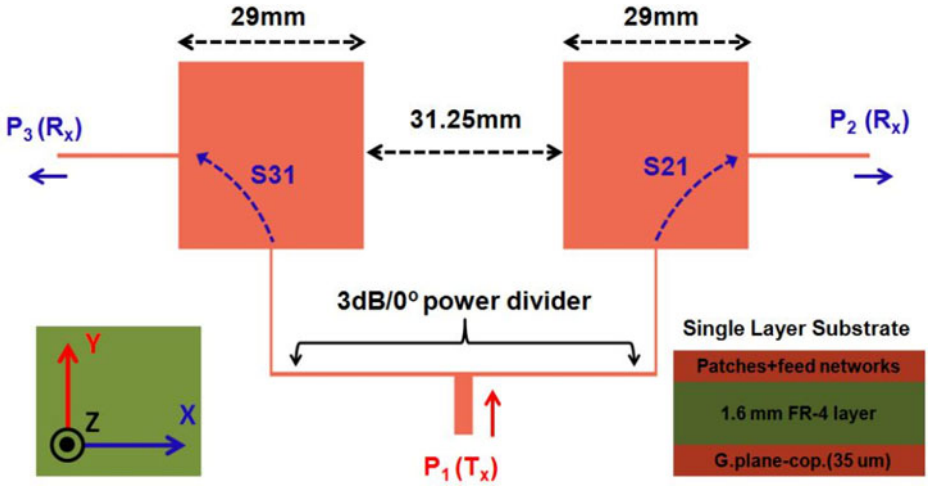


Fig. 3. The proposed 2.4 GHz dual polarized antenna array of two radiating patches with inter-element spacing of $\lambda_o/4 = 31.25$ mm (λ_o is the free space wavelength for 2.4 GHz frequency).

the realization of compact transceiver modules. Conversely, the IBFD transceiver based on monostatic antenna architecture (shared radiator for T_x and R_x operation) can be realized with a small form-factor (reduced size) to achieve all the potential gains of IBFD communication [16]. However, such a monostatic IBFD antenna system should provide high T_x–R_x interport isolation through SIC at the RF front end to prevent the saturation of analog to digital converter in the R_x chain from very strong RF signals of the co-located transmitter [9, 17].

Various techniques have been exploited previously in order to improve the interport isolation of monostatic antennas for IBFD applications. These techniques include polarization diversity [18–22] and hybrid techniques based on utilizing different modes and polarizations [23]. The techniques based on polarization diversity in conjunction with additional SIC approaches have attracted much attention in recent days to realize IBFD antennas with relatively compact dimensions (small form factors). Such monostatic antennas have dual polarized characteristics where horizontal and vertical polarizations (TM_{01} and TM_{10} modes) are excited through perpendicularly placed feeds. This basic configuration of this sort of polarization diversity provides ~35–40 dB isolation between T_x and R_x ports. The additional SIC approaches are be utilized with such dual polarized antennas for improved isolation. For instance, ~20 dB additional isolation has been achieved through a defected ground structure for the work reported in [24]. Moreover, multilayered printed patch antennas with hybrid feeding structures can provide 15–20 dB improvement in T_x–R_x isolation for IBFD applications [15, 25, 26]. In addition, differential feeding is one of the prominent SIC technique to achieve very nice interport isolation for dual polarized monostatic antennas [27–29]. The well-known signal inversion based analog/RF domain SIC techniques are also used with dual polarized antennas for isolation improvements [30–33]. For example, an RF-SIC circuit plus a circulator has been used in [33] to obtain >40 dB SIC for 65 MHz bandwidth.

In this paper, a dual-polarized 1 × 2 monostatic antenna array has been studied for 2.4 GHz applications where high T_x–R_x isolation has been achieved through well balanced differential feeding network at the R_x port. The proposed differential feeding at the R_x port effectively suppresses the RF leakage from the T_x port to present high interport isolation. A very simple 3 dB/180° ring hybrid coupler having nice amplitude and phase balance characteristics has been used for required differential feeding at the R_x port. The proposed differential feeding based SIC scheme has been mathematically described which achieves high T_x–R_x isolation without affecting the radiation characteristics of the presented antenna array. The effect of magnitude and phase imbalances of differential circuit on SIC levels is also illustrated analytically. A prototype of a compact 1 × 2 antenna array has been realized by implementing a dual polarized 1 × 2 antenna array with an integrated differential feeding network on a single layered printed circuit board (PCB). The implemented compact antenna array has been experimentally characterized. The measurement results demonstrate >30–35 dB additional isolation on the top of ~35 dB intrinsic isolation of polarization diversity for the dual polarized antenna array. The measured interport isolation for the implemented antenna array is >65 dB within a 10 dB return-loss impedance bandwidth of 50 MHz. In addition, the differential feeding at the R_x port suppresses the inter-element or mutual coupling to reduce side lobe levels (SLL).

The rest of this paper is organized as follows. Section "Differential feeding based SIC scheme for 1 × 2 IBFD antenna array" describes the array antenna architecture and describes the differential feeding based SIC topology for the proposed 1 × 2 array antenna. The proposed differential fed SIC scheme is also mathematically described in this section and dependence of SIC levels on characteristics of differential circuit is also illustrated. The design and simulation results for the compact differential fed array antenna are presented and discussed in section "Design and simulation results for compact differential fed 1 × 2 antenna array". The section "Measurement results for compact differential fed 1 × 2 IBFD antenna array" presents the test and measurement results for implemented prototype of the antenna array, followed by conclusions in section "Conclusion".

Differential feeding based SIC scheme for 1 × 2 IBFD antenna array

The proposed 2.4 GHz antenna array is shown in Fig. 3 which is comprised of two radiating patches with inter-element spacing of $\lambda_o/4 = 31.25$ mm where λ_o corresponds to the free space wavelength for 2.4 GHz frequency. The squared-shaped radiating elements characterize the same resonant frequencies of 2.4 GHz for T_x and R_x ports for intended IBFD operation. The proposed antenna array has been designed on a single layer, 1.6 mm thick FR-4 substrate ($\varepsilon_r = 4.4$, $\tan\delta = 0.02$) as illustrated in Fig. 3. The

https://doi.org/10.1017/S1759078719001569 Published online by Cambridge University Press

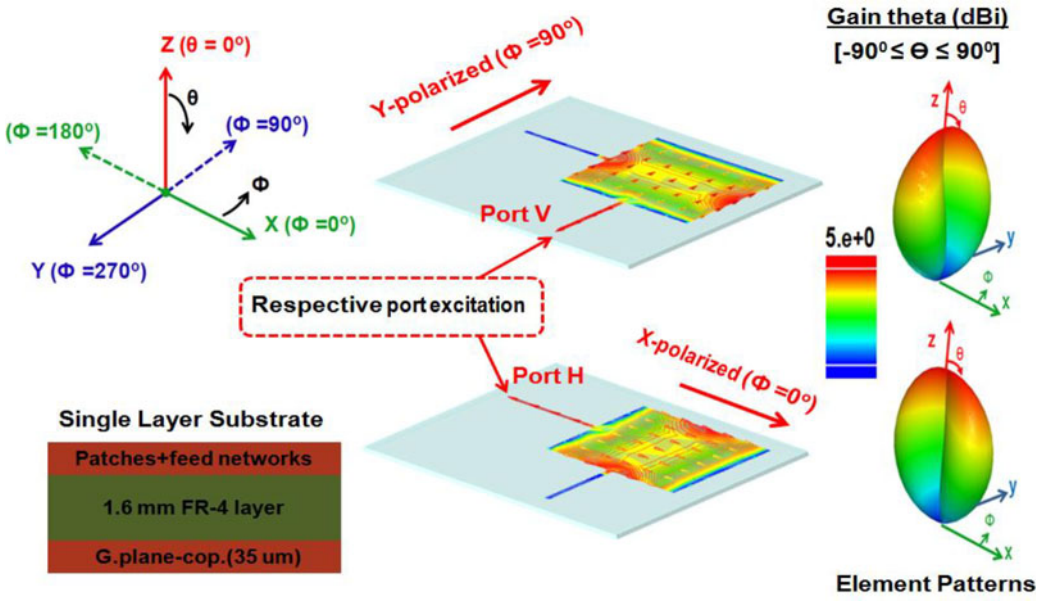


Fig. 4. The gain patterns and surface current distributions for dual polarized, single element (patch) of the proposed 1 × 2 antenna array (designed on a 1.6 mm thick FR-4 substrate).

optimized dimensions for the proposed array are also shown in Fig. 3. The symmetrically placed R_x ports with respect to the T_x port (through 3 dB/0° power divider) produce the same amount of SI from the T_x port to both R_x ports.

As clear from the structure of the proposed antenna array in Fig. 3, each radiating patch of array is excited from two orthogonally placed thin quarter-wave feeds which are connected at the center of the respective edge of the square-shaped patch. Consequently, each element will radiate with dual polarized characteristics when excited from respective T_x and R_x ports. This sort of feeding achieves the maximum T_x–R_x isolation at a required frequency through polarization diversity. This fact is illustrated and endorsed with simulated element gain patterns and surface current distributions for respective T_x/R_x port excitations as shown in Fig. 4.

Our proposed SIC scheme is based on employing a differential feeding through both R_x ports (P_2 and P_3) of the proposed dual polarized, 1 × 2 antenna array (which has been shown in Fig. 3) for effective suppression of SI resulted from the T_x port (P_1). The presented proposed SIC scheme achieves high T_x–R_x interport isolation without affecting the radiation characteristics (gain performance etc) of the antenna array as clear from following analysis. The phasor-form representation of linear polarized electric field vectors ($\boldsymbol{E}$) for T_x and R_x ports of the proposed dual polarized 1 × 2 antenna array (as presented in Fig. 3) can be expressed as:

$$\boldsymbol{E}_{Tx} = \boldsymbol{E}_{\boldsymbol{m}}\,(\hat{\boldsymbol{y}}) \quad \text{and} \quad \boldsymbol{E}_{Rx2} = \boldsymbol{E}_{\boldsymbol{m}}\,(\hat{\boldsymbol{x}}),\ \boldsymbol{E}_{Rx3} = \boldsymbol{E}_{\boldsymbol{m}}\,(-\hat{\boldsymbol{x}}) \tag{3}$$

As stated earlier, our proposed SIC scheme is based on differential excitation of both R_x ports (P_2 and P_3) of the proposed dual polarized 1 × 2 antenna array, in that case, the electric field vector ($\boldsymbol{E}$) for the differential fed R_x mode can be expressed as:

$$\boldsymbol{E}_{R_x} = \boldsymbol{E}_{Rx2} + \mathrm{e}^{j180^\circ}\boldsymbol{E}_{Rx3} = \boldsymbol{E}_{\boldsymbol{m}}(\hat{\boldsymbol{x}}) - \boldsymbol{E}_{\boldsymbol{m}}\,(-\hat{\boldsymbol{x}}) = 2 \times \boldsymbol{E}_{\boldsymbol{m}}\,(\hat{\boldsymbol{x}}) \tag{4}$$

where $\hat{\boldsymbol{x}}$ and $\hat{\boldsymbol{y}}$ are unit vectors along x and y respectively and $\boldsymbol{E}_{\mathrm{m}}$ is the amplitude of $\boldsymbol{E}$ field.

As clear from (4), the fields radiated by both elements of the array antenna are combined in phase when differential feeding through both R_x ports of the proposed antenna array is employed. Consequently, the presented 1 × 2 antenna array with differential R_x mode will transmit and receive with vertical and horizontal polarizations respectively as clear from (3) and (4).

The SIC capabilities of the proposed scheme for the dual polarized 1 × 2 antenna array can be described through very simple mathematical analysis as follows. We assume that I_{Tx}, I_{Rx2}, and I_{Rx3} denote the currents for respective T_x and R_x ports as indicated in Fig. 3, then:

$$I_{Rx2} = I_{T_x}\,S_{21} \quad \text{and} \quad I_{Rx3} = I_{T_x}\,S_{31} \tag{5}$$

For differential excitation, the total current I_{Rx} flowing out from the differential R_x port is:

$$I_{Rx} = \frac{1}{\sqrt{2}}(e^{j180^\circ}I_{Rx2} + I_{Rx3}) = \frac{I_{Tx}}{\sqrt{2}}(\,S_{31} - S_{21}) \tag{6}$$

The T_x–R_x interport current isolation (inverted current coupling ratio) is given as:

$$\frac{I_{Tx}}{I_{Rx}} = \frac{1}{(S_{31} - S_{21})} \tag{7}$$

As stated earlier and clear from Fig. 3, the same levels of RF coupling (SI) is resulted from the T_x port to both R_x ports due to symmetry of the proposed structure for the dual polarized antenna array. In other words $S_{21} = S_{31}$ to offer infinite T_x–R_x interport isolation theoretically based on mathematically established SIC condition in (7). However, for practical differential fed, dual polarized antenna array $S_{21} \approx S_{31}$ (due to the non-ideal layout and imperfect excitations) and high levels of SIC can be achieved when a differential circuit having nice amplitude and phase balance characteristics are employed with the proposed dual polarized antenna array. In addition, the differential feeding suppresses the mutual coupling

https://doi.org/10.1017/S1759078719001569 Published online by Cambridge University Press

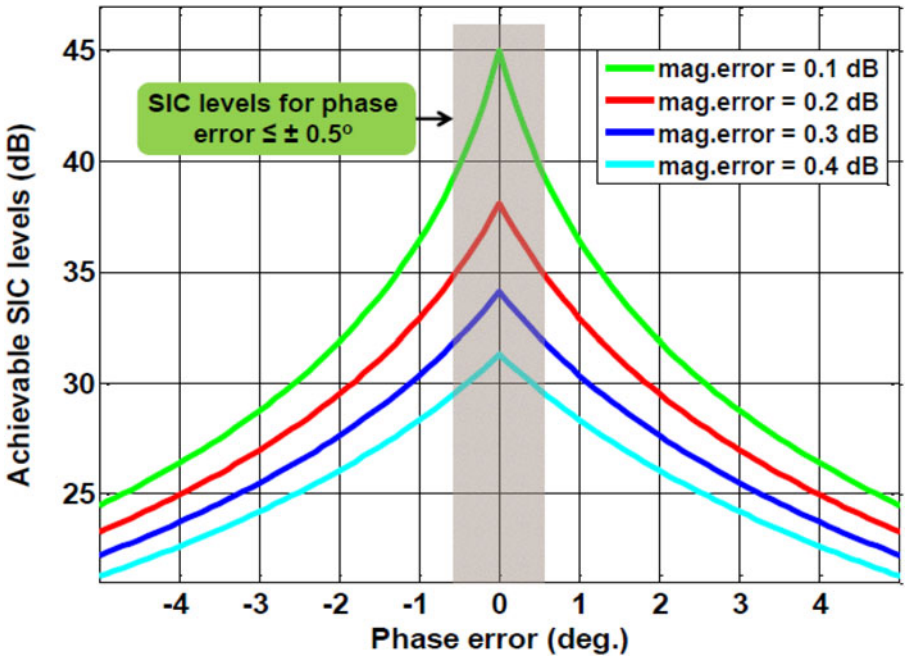


Fig. 5. The computed SIC levels under various magnitude & phase errors between two signals.

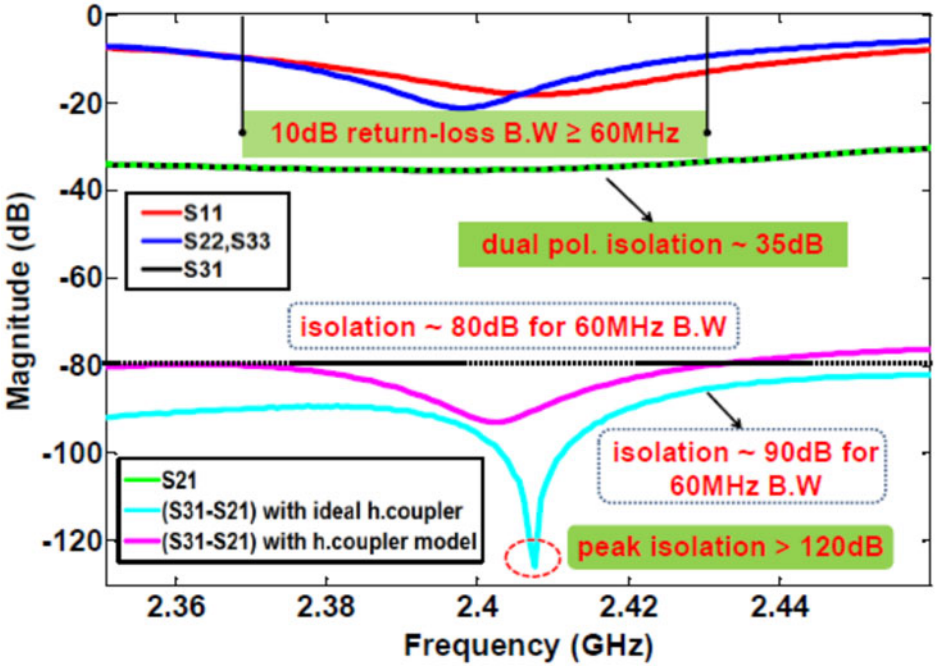


Fig. 6. The simulated return loss (S_{11}, S_{22}, and S_{33}) and interport isolation (S_{21}, S_{31}, and S_{31}–S_{21}) results for the proposed 1 × 2 dual polarized 2.4 GHz antenna array.

between antenna elements which improves antenna gain and polarization purity through reduced SLL levels [34].

The achievable SIC levels and T_x–R_x isolation bandwidth are highly dependent on characteristics of the employed differential feeding network (circuit). This dependence can be quantitatively analyzed for SIC levels for two equal-magnitudes out of phase sinusoidal signals. Figure 5 presents the computed SIC levels under various magnitude and phase errors between two signals. The achieved levels of SIC are greatly influenced by both magnitude and phase errors between two signals which corresponds to magnitude and phase imbalances of the differential feeding network. For instance, as illustrated in Fig. 5, the SIC levels are reduced from 45 to 30 dB when phase error is varied from 0 to ±2° for 0.1 dB magnitude error curve. Similarly, if magnitude error is increased from 0.1 to 0.3 dB, the corresponding SIC levels are reduced from 45 to 35 dB with zero phase error in both cases. We have used a 3 dB/180° ring hybrid coupler as a differential circuit with nice amplitude and phase balance characteristics to achieve improved SIC levels for the proposed differential fed antenna array.

Design and simulation results for compact differential fed 1 × 2 antenna array

The simulated return-loss (S_{11}, S_{22}, and S_{33}) and interport isolation results (S_{21}, S_{31}, and S_{31}–S_{21}) for the 1 × 2 antenna array are presented in Fig. 6. As stated earlier and clear from simulation

https://doi.org/10.1017/S1759078719001569 Published online by Cambridge University Press

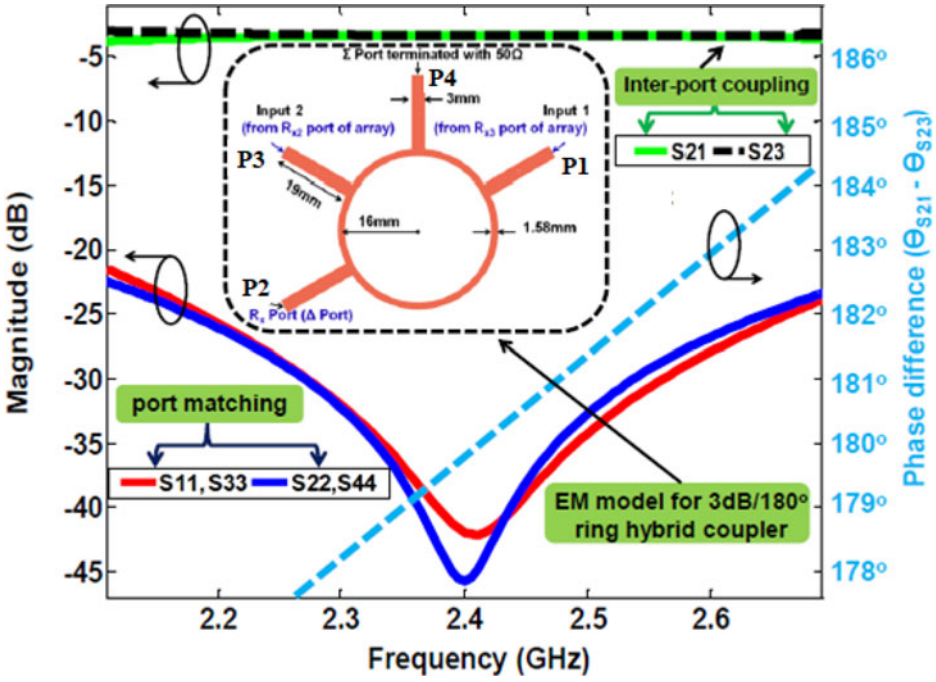


Fig. 7. EM model and simulation results for the 3 dB/180° ring hybrid coupler (SIC circuit). The coupler has been designed on a 1.6 mm thick FR-4 substrate ($\varepsilon_r = 4.4$ & $\tan\delta = 0.02$).

results in Fig. 6, the polarization diversity provides ~35 dB interport isolation (S_{21}, S_{31}) for the presented antenna array. The differential feeding through both R_x ports can provide additional isolation as clear from (S_{31}–S_{21}) results in Fig. 6. The ideal differential feeding network (having zero magnitude and phase errors) can demonstrate peak T_x–R_x interport isolation >120 dB and around 90 dB isolation in 60 MHz. However, better than 80 dB isolation in 60 MHz is achieved with our proposed hybrid coupler as a differential circuit as clear from Fig. 6.

The intended differential R_x mode operation has been realized by using a 2.4 GHz, 3 dB/180° ring hybrid coupler. The ring hybrid coupler performs as a 3 dB out of phase power combiner for required SIC operation when it is connected with the proposed array where a difference port (Δ port) designated as P_2 of the hybrid coupler is used for the R_x port as indicated in Fig. 7.

A 2.4 GHz, 3 dB/180° ring hybrid coupler has been designed on a 1.6 mm thick general purpose FR-4 substrate ($\varepsilon_r = 4.4$, $\tan\delta = 0.02$) and optimized design parameters for the 2.4 GHz 3 dB/180° ring hybrid coupler are shown in Fig. 7. The simulation results for the 2.4 GHz, 3 dB/180° ring hybrid coupler are also shown in Fig. 7. The proposed 2.4 GHz 3 dB/180° ring hybrid coupler provides very nice port matching and amplitude balance characteristics as clear from Fig. 7. The simulated return-loss for each port >20 dB over the frequency range of 2.1 to 2.7 GHz. Moreover, the simulation results indicate <0.1 dB amplitude imbalance and $< \pm 1°$ phase difference for the frequency range of 2.35 to 2.45 GHz (100 MHz bandwidth). As stated earlier and shown in Fig. 5, a differential network (circuit) with these values of amplitude and phase errors will offer >35 dB SIC over 100 MHz on the top of 30–35 dB isolation (polarization diversity isolation). Hence, the total interport isolation should fall in the range of 65–70 dB over a SIC bandwidth of 100 MHz. However, the SIC levels will improve when the SIC bandwidth is reduced because of comparatively small amplitude and phase errors. Moreover we need to perform SIC in 60 MHz bandwidth only as our proposed antenna array has 10 dB return-loss bandwidth of 60 MHz (as clear from Fig. 6).

As presented in Fig. 8, the three port antenna array and 3 dB/180° power combiner are integrated to realize a compact antenna structure for a single-input single-output IBFD transceiver. This design has been realized on a single-layered 1.6 mm thick general purpose FR-4 substrate ($\varepsilon_r = 4.4$, $\tan\delta = 0.02$). The radiating structure (antenna elements) and differential feeding network are placed on top of the FR-4 substrate whereas the copper layer on the bottom side of the substrate will form a ground plane for the presented patch antenna array as indicated in Fig. 8. The microstrip transmission lines have been used for intended interconnections. As shown in Fig. 8 through full-wave simulated surface currents for individual excitation of T_x and R_x ports, the presented differential fed patch antenna array is linearly vertically and horizontal polarized for excitation from respective T_x and R_x ports. As clear from Fig. 8, the difference port (Δ port) of the integrated 2.4 GH, 3 dB/180° ring hybrid coupler has been used as the R_x port of the compact, dual polarized IBFD antenna array for effective SIC operation which is based on differential feeding at the R_x port as detailed earlier in section "Differential feeding based SIC scheme for 1 × 2 IBFD antenna array".

Measurement results for compact differential fed 1 × 2 IBFD antenna array

The proposed dual polarized, differential fed, 1 × 2 antenna array was implemented and measured in order to verify the differential feeding based SIC concept. A single-layered FR-4 substrate ($\varepsilon_r = 4.4$, $\tan\delta = 0.02$) having with a thickness of 1.6 mm was used for the implementation of the prototype of the proposed array. The implemented validation model for the compact (array and feeding networks on the same PCB), dual port, dual polarized, differential fed IBFD antenna array is shown in Fig. 9. The designated T_x and R_x ports and detailed dimensions for the implemented prototype of the antenna array are also shown in Fig. 9. Three SMA

https://doi.org/10.1017/S1759078719001569 Published online by Cambridge University Press

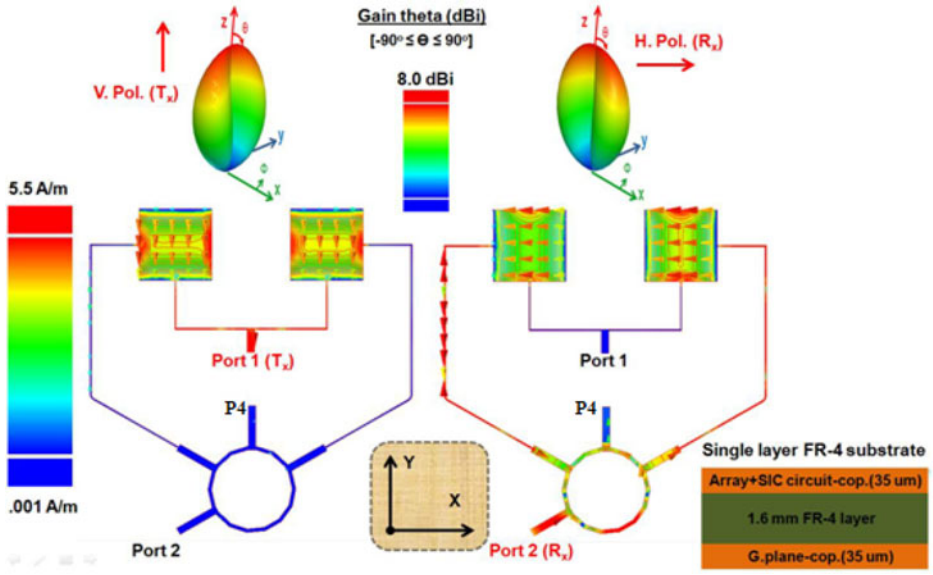


Fig. 8. The simulated surface current distributions at 2.4 GHz frequency for the compact, differential fed, dual polarized 1 × 2 IBFD antenna array.

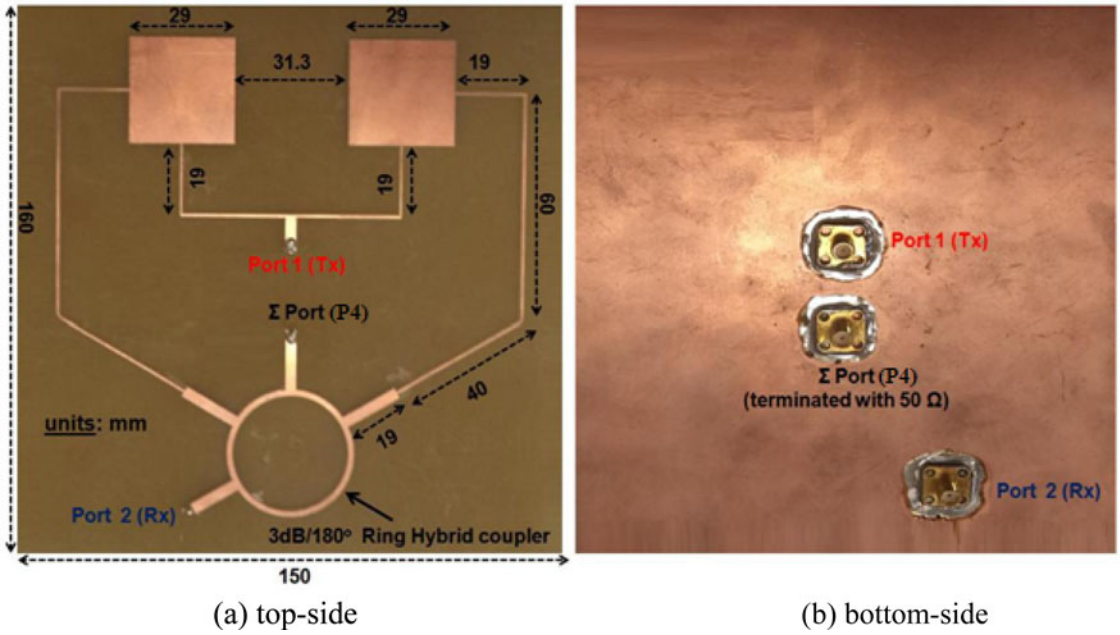


Fig. 9. The implemented prototype of the compact, dual port, dual polarized, differential fed 1 × 2 array antenna for 2.4 GHz full duplex wireless applications.

connectors (two for T_x and R_x ports and one for 50 Ω termination at Σ port of the ring hybrid coupler) were soldered on the back side of the PCB and connected to respective ports as shown in Fig. 9.

The implemented antenna array has been characterized by measuring the input reflection coefficients (S_{11}, S_{22}) and interport coupling (negative isolation). Figure 10 plots the measured and simulated impedance matching (S_{11}, S_{22}) and T_x–R_x coupling (S_{21}) performance results for the implemented validation model of the differential fed, dual polarized, 1 × 2 IBFD antenna array. The measured impedance bandwidth (referring to return loss ≥10 dB) for port 1 (T_x port) ≥50 MHz (from 2.39 to over 2.44 GHz) and >45 MHz (from 2.39 to 2.435 GHz) for port 2 (R_x port). Meanwhile, very high T_x–R_x isolation levels have been observed where the measured peak T_x–R_x isolation levels ~85 dB as illustrated in Fig. 10. Moreover, the measured isolation (in chamber) is over 65 dB within 50 MHz (2.39 to 2.44 GHz) and better than 75 dB in 20 MHz (2.4 to 2.42 GHz). The interport measurement results reflect a nice SIC performance through differential feeding at the R_x port.

As discussed earlier, the dual polarization provides 35–40 dB isolation between T_x and R_x signals and our proposed SIC scheme based on differential R_x operation has achieved 30–35 dB additional isolation on top of polarization diversity isolation. As clear from Fig. 10, there is nice agreement between the simulation and measurement results performed in an anechoic chamber. However, the measured isolation results show some degradations compared to simulated one, which can be attributed to fabrication accuracy. The measured isolation in a lab environment (in the presence of reflections) is >65 dB for 50 MHz bandwidth.

https://doi.org/10.1017/S1759078719001569 Published online by Cambridge University Press

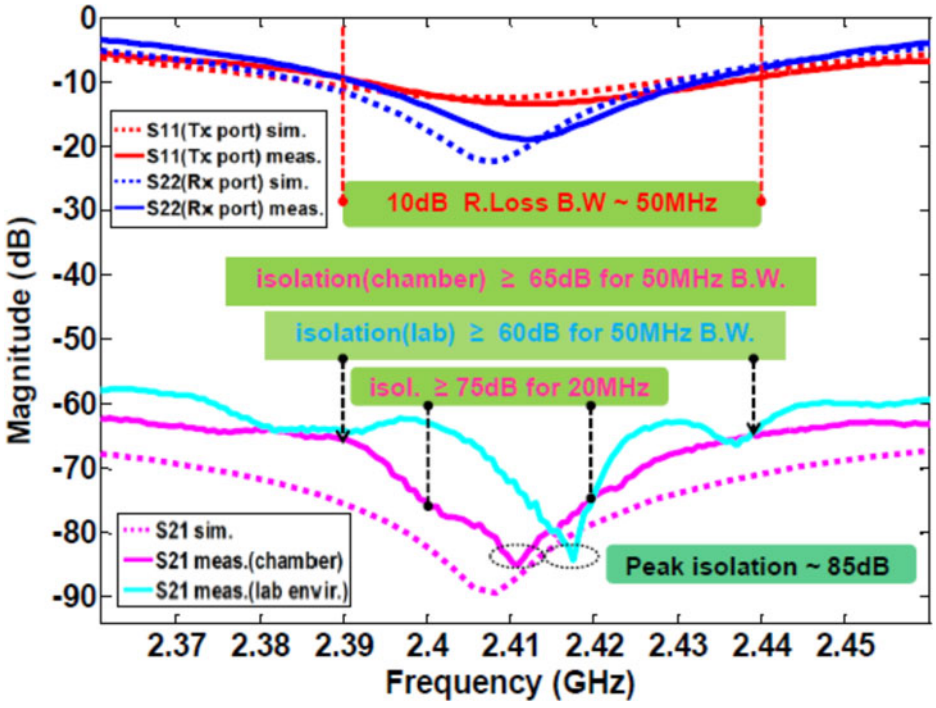


Fig. 10. The simulated and measured *S*-parameters ($_{S11}$, $_{S22}$, and S_{21}) result for the implemented prototype of the dual port, dual polarized, and differential fed IBFD antenna array.

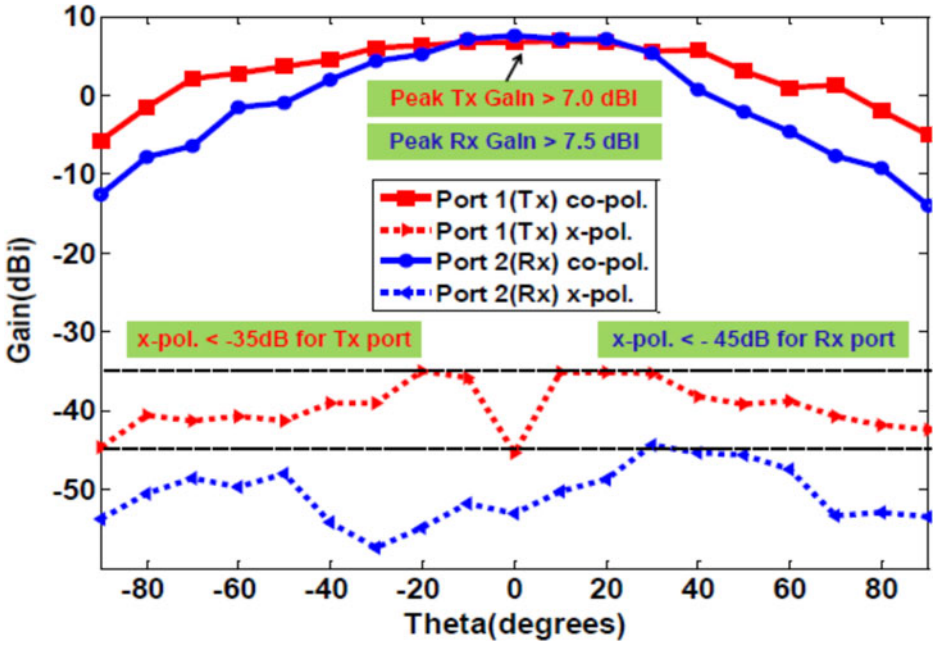


Fig. 11. The measured E-plane, 2-D far-field radiation patterns at 2.4 GHz frequency for the implemented prototype of the dual polarized, differential fed antenna array.

The measured E-plane far-field, two-dimensional (2-D) radiation patterns at 2.4 GHz frequency for the implemented prototype of the dual port, differential fed array antenna are depicted in Fig. 11. The implemented validation model of the dual polarized array characterizes >7 and >7.5 dBi gains for linear dual polarized radiations under port 1 (T_x port) and port 2 (R_x port) excitations respectively. The simulated radiation efficiency (not presented here for brevity) is around 50% only for each port excitation and gain/efficiency for the array can be improved by using low loss substrate instead of the general purpose FR-4 substrate (with $\tan\delta = 0.02$). Moreover, the measured cross-polarization levels at the boresight are lower than −35 dB (T_x port) and −45 dB (R_x port) from respective co-polarized levels as illustrated in Fig. 11. These measurement results reflect nice polarization purity characteristics for the implemented array.

The radiation efficiency of the presented antenna is low due to high loss (loss tangent) of FR-4 dielectric used for array antenna implementation. The radiation efficiency and consequently the gain of the presented antenna array can be improved significantly by using a low loss substrate for antenna implementation. This can be endorsed through antenna array simulations with reduced value loss tangent ($\tan\delta$). For example, as reported in [35] and clear from simulation results in Fig. 12, the radiation efficiency of the antenna will be increased to more than 87% at 2.4 GHz

https://doi.org/10.1017/S1759078719001569 Published online by Cambridge University Press

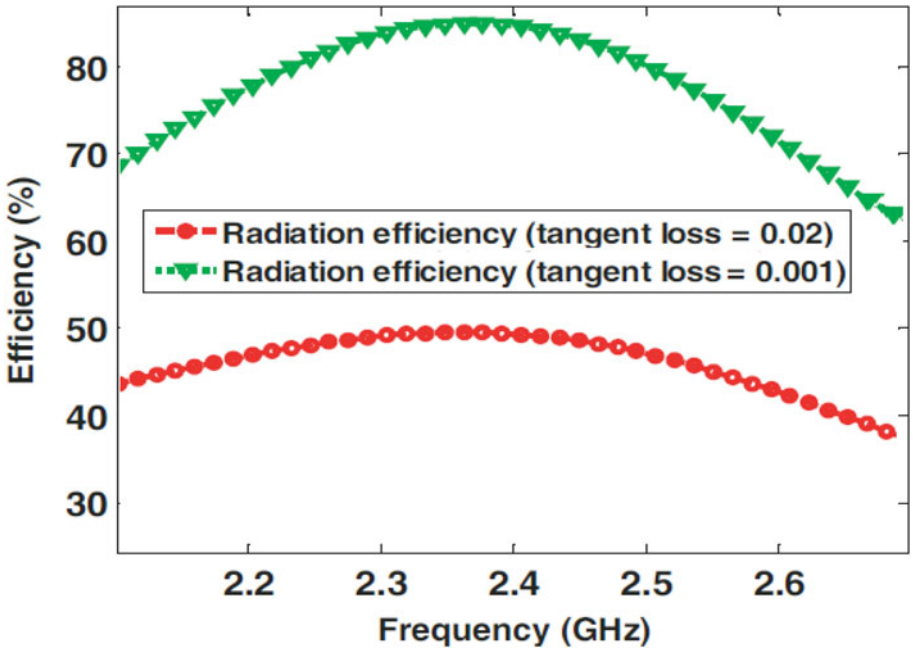


Fig. 12. The simulated radiation efficiencies of the presented antenna for tan $\delta = 0.02$ & tan $\delta = 0.001$ when the R_x port of the proposed antenna array is excited.

Table 1. Performance comparison of the implemented antenna array with previously published works [25, 27, 29, 35]

Antennas	Peak isolation (dB)	10 dB R.L.B.W.	Isolation/B.W.	PCB configuration
[25]	33	18.8%	28 dB/410 MHz	Multi-layered
[27]-Ant.1	67	50 MHz	62 dB/50 MHz	Single-layered
[27]-Ant.2	90	50 MHz	70 dB/50 MHz	Multi-layered
[29]	98	50 MHz	80 dB/40 MHz 90 dB/20 MHz	Multi-layered
[35]	78	50 MHz	64 dB/50 MHz	Single-layered
This work	85	50 MHz	65 dB/50 MHz 75 dB/20 MHz	Single-layered

frequency when tanδ is reduced from 0.02 to 0.001. Consequently the gain of the antenna will be doubled (3 dB additional gain in this case).

The measured results for the implemented prototype of the proposed array (especially interport isolation results) demonstrate improved performance compared to previously published works on such antennas [25, 27, 29, 35]. These performance improvements are attributed to effective cancellation of mutual coupling and SI through a well-balanced differential feeding mechanism. The comparison of the presented antenna with previously reported 2.4 GHz antennas is detailed in Table 1. As listed in Table 1, the reported antenna array in [25] provides a wider bandwidth of 18.8% but the interport isolation is limited to around 28 dB for this topology. Moreover, it employs the multi-layered PCB configuration. Our previously reported antennas in [27, 29, 35] are based on differential feeding through similar ring hybrid couplers. However, these antennas are based on single radiating element where mutual coupling is not an issue and differential feeding is only intended for improved interport isolation. Moreover, the second antenna in [27] and double differential antenna reported in [29] require multi-layered PCB structures. Compared to previously reported antennas, the novelty of the presented antenna is single-layered antenna array architecture (reduced implementation complexity) and very high interport isolation through effective reduction and cancellation of inter-element coupling (mutual coupling) and T_x leakage at the R_x port. Compared to the single element based antenna, the array antenna configuration with comparable interport isolation performance is more useful for full duplex wireless applications as it provides more gain to extend the range or coverage for specified T_x power. However, the mutual coupling degrades the radiation performance and interport isolation of the IBFD antenna array. The presented antenna configuration resolves this issue through a well-balanced differential R_x mode operation.

Conclusion

In this work, a differential fed 1 × 2 dual-polarized antenna array has been presented for 2.4 GHz IBFD applications. The differential feeding mechanism at the R_x port has been realized through a very simple 3 dB/180° ring hybrid coupler having nice amplitude and phase balance characteristics. The proposed SIC topology achieves high interport isolation through the combination of polarization diversity and differential feeding mechanism at the

https://doi.org/10.1017/S1759078719001569 Published online by Cambridge University Press

R_x port of the proposed antenna array. The differential mechanism also improves the antenna radiation performance with reduced SLL through reduction in mutual coupling between antenna elements for R_x operational mode. The measurement results indicate very high SIC levels for implemented prototype of the monostatic antenna array. The measured interport isolation performance ensures that the implemented prototype of the monostatic antenna array can be effectively used for 2.4 GHz IBFD wireless applications where the independence of the T_x and R_x channels corresponds to the high interport isolation. For instance, the proposed antenna array can be used for simultaneous wireless power transfer and data reception from wireless sensor devices through two independent wireless channels working at the same frequency band.

References

1. **Sabharwal A, Schniter P, Guo D, Bliss DW, Rangarajan S and Wichman R** (2014) In-band full-duplex wireless: challenges and opportunities. *IEEE Journal on Selected Areas in Communications* **32**, 1637–1652.
2. **Bharadia D, McMilin E and Katti S** (2013) Full Duplex Radios, ACM SIGCOMM 2013, Hong Kong.
3. **Maraševic J, Zhou J, Krishnaswamy H, Zhong Y and Zussman G** (2017) Resource allocation and rate gains in practical full-duplex systems. *IEEE/ACM Transactions on Networking* **25**, 292–305.
4. **Heino M, Venkatasubramanian SN, Icheln C and Haneda K** (2016) Design of wavetraps for isolation improvement in compact in-band full-duplex relay antennas. *IEEE Transactions on Antennas and Propagation* **64**, 1061–1070.
5. **Mao C, Gao S and Wang Y** (2018) Dual-band full-duplex T_x/R_x antennas for vehicular communications. *IEEE Transactions on Vehicular Technology* **67**, 4059–4070.
6. **Li R, Masmoudi A and Ngoc TL** (2018) Self-interference cancellation with nonlinearity and phase-noise suppression in full-duplex systems. *IEEE Transactions on Vehicular Technology* **67**, 2118–2129.
7. **Liao Y, Song L and Han Z** (2014) Full-Duplex Wireless Communication and Networks: Key Technologeis and Applications. *IEEE International Conference on Communications in China (ICCC 2014)*, Shanghai, China.
8. **Choi JI, Jain M, Srinivasan K, Levis P and Katti S** (2010) Achieving single channel full duplex wireless communication. *Proc. 16th Annual International Conference on Mobile Computing and Networking*, pp. 1–12.
9. **Korpi D, Riihonen T, Syrjälä V, Anttila L, Valkama M and Wichman R** (2014) Full-duplex transceiver system calculations: analysis of ADC and linearity challenges. *IEEE Transactions on Wireless Communications* **13**, 3821–3836.
10. **Anttila L, Korpi D, Syrjälä V and Valkama M** (2013) Cancellation of power amplifier induced nonlinear self-interference in full-duplex transceivers. 2013 Asilomar Conference on Signals, Systems and Computers, Pacific Grove, CA, pp. 1193–1198.
11. **Hong S, Brand J, Choi J, Jain M, Mehlman J, Katti S and Levis P** (2014) Applications of self-interference cancellation in 5 G and beyond. *IEEE Communications Magazine* **52**, 114–121.
12. **Nawaz H and Tekin I** (2017) Compact dual-polarized microstrip patch antenna with high interport isolation for 2.5 GHz in-band full-duplex wireless applications. *IET Microwaves, Antennas & Propagation* **11**, 976–981.
13. **van den Broek D-J, Klumperink E and Nauta B** (2015) A self-interferencecancelling receiver for in-band full-duplex wireless with low distortion under cancellation of strong TX leakage. *IEEE Int. Solid-State Circuits Conf. (ISSCC) Dig. Tech. Papers*, pp. 1–3.
14. **Amjad MS, Nawaz H, Özsoy K, Gürbüz Ö and Tekin I** (2018) A low-complexity full-duplex radio implementation with a single antenna. *IEEE Transactions on Vehicular Technology* **67**, 2206–2218.
15. **Nawaz H and Tekin I** (2016) Three dual polarized 2.4 GHz microstrip patch antennas for active antenna and in-band full duplex applications. *2016 16th Mediterranean Microwave Symposium (MMS)*, Abu Dhabi, United Arab Emirates, pp. 1–4.
16. **Knox ME** (2012) Single antenna full duplex communications using a common carrier. *IEEE 13th Annual Wireless and Microwave Technology Conference*, pp. 1–6.
17. **Duarte M, Dick C and Sabharwal A** (2012) Experiment-driven characterization of full-duplex wireless systems. *IEEE Transactions on Wireless Communications* **11**, 4296–4307.
18. **Wu J, Cheng YJ and Fan Y** (2016) Wide-band dual-polarized planar array antenna for K/Ka-band wireless communication. *Microwave and Optical Technology Letters* **58**, 2377–2381.
19. **Wong H, Lau K-L and Luk K-M** (2004) Design of dual-polarized L-probe patch antenna arrays with high isolation. *IEEE Transactions on Antennas and Propagation* **52**, 45–52.
20. **Gao S and Sambell A** (2005) Dual-polarized broad-band microstrip antennas fed by proximity coupling. *IEEE Transactions on Antennas and Propagation* **53**, 526–530.
21. **Li Y, Zhang Z, Chen W, Feng Z and Iskander MF** (2010) A dualpolarization slot antenna using a compact CPW feeding structure. *IEEE Antennas and Wireless Propagation Letters* **9**, 191–194.
22. **Zhou S-G, Huang G-L, Chio T-H, Yang J-J and Wei G** (2015) Design of a wideband dual-polarization full-corporate waveguide feed antenna array. *IEEE Transactions on Antennas and Propagation* **63**, 4775–4782.
23. **Etellisi EA, Elmansouri MA and Filipovic DS** (2017) Wideband multimode monostatic spiral antenna STAR subsystem. *IEEE Transactions on Antennas and Propagation* **65**, 1845–1854.
24. **Younkyu C, Seong-Sik J, Ahn D, Jae-Ick C and Itoh T** (2004) High isolation dual-polarized patch antenna using integrated defected ground structure. *IEEE Microwave & Wireless Components Letters* **14**, 4–6.
25. **Deng C, Li Y, Zhang Z and Feng Z** (2014) A wideband high-isolated dual-polarized patch antenna using two different balun feedings. *IEEE Antennas & Wireless Propagation Letters* **13**, 1617–1619.
26. **Rikuta Y and Arai H** (2002) A self-diplexing antenna using slitted patch antenna. *Proceedings of the International Symposium on Antennas and Propagation* Japan.
27. **Nawaz H and Tekin I** (2017) Dual-polarized, differential fed microstrip patch antennas with very high interport isolation for full-duplex communication. *IEEE Transactions on Antennas and Propagation* **65**, 7355–7360.
28. **Xie JJ, Yin YZ, Wang JH and Liu XL** (2013) Wideband dual-polarized electromagnetic fed patch antenna with high isolation and low cross-polarization. *Electronic Letters* **49**, 171–173.
29. **Nawaz H and Tekin I** (2018) Double differential fed, dual polarized patch antenna with 90 dB interport RF isolation for 2.4 GHz in-band full duplex transceiver. *IEEE Antennas and Wireless Propagation Letters* **17**, 287–290.
30. **Kolodziej K, McMichael J and Perry B** (2016) Multitap RF canceller for in-band full-duplex wireless communications. *The IEEE Transactions on Wireless Communications* **15**, 4321–4334.
31. **Nawaz H and Tekin I** (2016) Dual port single patch antenna with high interport isolation for 2.4 GHz in-band full duplex wireless applications. *Microwave and Optical Technology Letters* **58**, 1756–1759.
32. **Nawaz H and Tekin I** (2016) Dual polarized patch antenna with high inter-port isolation for 1 GHz in-band full Duplex applications. *2016 IEEE International Symposium on Antennas and Propagation (APSURSI)*, Fajardo, PR, USA, pp. 2153–2154.
33. **Khaledian S, Farzami F, Smida B and Erricolo D** (2018) Inherent self-interference cancellation for in-band full-duplex single-antenna systems. *IEEE Transactions on Microwave Theory and Techniques* **66**, 2842–2850.
34. **Liang X-L, Zhong S-S and Wang W** (2005) Design of a dual-polarized microstrip patch antenna with excellent polarization purity. *Microwave and Optical Technology Letters* **44**, 329–331.
35. **Nawaz H and Basit MA** (2019) Single layer, dual polarized, 2.4 GHz patch antenna with very high RF isolation between DC isolated T_x-R_x ports for full duplex radio. *Progress In Electromagnetics Research Letters* **85**, 65–72.

https://doi.org/10.1017/S1759078719001569 Published online by Cambridge University Press



Haq Nawaz received the B.Sc. degree in Electrical Engineering and the Master's degree in Telecommunication Engineering from the University of Engineering and Technology (UET), Taxila, Pakistan, in 2005 and 2012, respectively. He received the Ph.D. degree in Electronic Engineering from Sabanci University, Istanbul, Turkey. From January, 2017 to June, 2018, he has worked as a post-doc research fellow with Faculty of Engineering and Natural Sciences (FENS), Sabanci University, Turkey. During 2006–2009, he was with SUPARCO Pakistan as a RF Design Engineer. He served UET Taxila, Sub-campus Chakwal, Pakistan, as a Lecturer in Electronics Engineering from 2010 to 2012.

Currently, he is working as an Assistant Professor at department of Electronics Engineering, UET Taxila, Sub-campus Chakwal, Pakistan. His research interests include full duplex antenna design, RF circuits design and measurements for Radar and Satellite systems, beam-switched and phased scanning array antennas design, and indoor positioning systems design.



Ahmad Umar Niazi received the B.Sc. degree in Electrical Engineering with specialization in Communication & Electronics from the University of Engineering & Technology (UET), Lahore, Pakistan and the Master's degree in Electrical Engineering from the University of Engineering and Technology (UET), Taxila, Pakistan, in 2001 and 2012, respectively. He is now pursuing his Ph.D. degree in Electrical Engineering from UET Taxila, Pakistan. He served at private and public sector industries/organizations from 2001 to 2006. He joined UET Taxila, Sub-campus Chakwal, Pakistan, and served as a Lecturer in Electronics Engineering from 2007 to 2012.

Since 2012, he is working as an Assistant Professor at department of Electronics Engineering, UET Taxila, Sub-campus Chakwal, Pakistan. His research interests include microwave antenna design, antennas for 5 G applications, full duplex antenna design, RF circuits design, beam-switched and phased scanning array antennas, and multi-band jamming techniques.



Muhammad Abdul Basit received the B.S. degree in telecommunication engineering from FAST NUCES Islamabad, the M.S. degree in electrical engineering from UET Taxila, and the Ph.D. degree in communication and information engineering from the University of Electronic Science and Technology of China (UESTC), in 2016.

He has been an Assistant Professor with the Department of Electronics Engineering, UET Taxila, Sub-Campus Chakwal, since 2007. His area of specialization in the Ph.D. was antenna design. His research interests include flush mounted antenna design, dual polarized antenna design, and phased scanning array antennas.



Furqan Shaukat is currently working as an Assistant Professor in Department of Electronics Engineering UET Taxila Sub Campus Chakwal. He completed his BSc in Electrical Engineering from UET Lahore in 2007. He received his M.Sc. and Ph.D. degrees from UET Taxila in 2011 and 2018 respectively. He has also worked as a Research Associate in University of Sheffield UK during his Ph.D. His research interests include computer vision and full duplex wireless communication.



Muhammad Usman received the B.Sc. and M.Sc. degrees in Electrical Engineering from University of Engineering and Technology Taxila (UET Taxila) Pakistan in 2005 and 2012 respectively. He worked in Attock Refinery Ltd. (ARL) as a trainee engineer from January 2007 to January 2008. He then joined Pakistan Telecommunication Company Limited (PTCL) in March 2008 and served as a Senior Engineer till April 2013. In April 2013, he joined Department of Electronics Engineering in UET Taxila, sub-campus Chakwal as an Assistant Professor and is associated with teaching and research activities. His current research interests include Optical Communications and Optical Networks and Antenna System Design. Muhammad Usman is a member of Pakistan Engineering Council (PEC).

https://doi.org/10.1017/S1759078719001569 Published online by Cambridge University Press